Kinetic enhancement in photocatalytic oxidation of organic compounds by WO₃ in the presence of Fenton-like reagent

Hongshin Lee [a,b,1], Jihyun Choi [a,1], Seokheon Lee [a], Seong-Taek Yun [c], Changha Lee [b,*], Jaesang Lee [a,**]

[a] Water Resource Cycle Center, Korea Institute of Science and Technology (KIST), Hwarangno 14-gil 5, Seongbuk-gu, Seoul 136-791, Republic of Korea
[b] School of Urban and Environmental Engineering, Ulsan National Institute of Science and Technology (UNIST), 100 Banyeon-ri, Eonyang-eup, Ulju-gun, Ulsan 698-805, Republic of Korea
[c] Department of Earth and Environmental Sciences, Korea University, 145 Anam-ro, Seongbuk-gu, Seoul 136-701, Republic of Korea

ABSTRACT

WO₃-mediated photocatalytic oxidation is achievable in the presence of electron acceptors as an alternative to O_2 or co-catalysts enabling O_2 reduction pathway. This study suggests the combination with Fenton-like reagent (Fe(III)/H_2O_2) as a strategy to improve the photocatalytic activity of WO₃. Under neutral pH condition where Fe(III) is present as iron oxide precipitate, photocatalytic degradation of 4-chlorophenol (4-CP) proceeded 3-fold faster in the WO₃/Fe(III)/H_2O_2 system relative to the WO₃/H_2O_2 system, while no noticeable oxidation occurred in the systems of Fe(III)/H_2O_2, WO₃, and WO₃/Fe(III). Such efficacy increase at circumneutral pH was observed in photocatalytic oxidation of diverse organics including phenol, bisphenol A, acetaminophen, and carbamazepine. Compatible with the pH dependence of photocatalytic activity of the WO₃/Fe(III)/H_2O_2 system, hydroxylation of benzoic acid and coumarin as indirect indication for OH radical production was drastically retarded with increasing pH. The pH effect indicates that OH radical as primary oxidant may be responsible for the kinetic enhancement in the WO₃/Fe(III)/H_2O_2 system. In that platinum deposits or Nafion layers as physical barriers possibly inhibit surface Fe(III) precipitation, use of platinized or Nafion-coated WO₃ caused the negligible photocatalytic improvement in the ternary system. Effective oxidative degradation in the presence of the UV cut-off filter corroborated visible light activation of the WO₃/Fe(III)/H_2O_2 system.

© 2013 Elsevier B.V. All rights reserved.

1. Introduction

The strong oxidizing power of photo-generated oxidants (e.g., valence band (VB) hole and hydroxyl radical ($^\bullet$OH)) and relatively low energy input required to drive photosensitized reactions allow selected metal oxide semiconductors (e.g., TiO_2, ZnO, and WO₃) to be applied as environmental photocatalyst for the degradation of a diverse range of organic contaminants in water [1–3]. Since the interfacial charge transfer is in competition with the recombination of electron–hole pairs, the presence of chemical additives (e.g., Cu(II), Fe(III), and polyoxometalates) as electron acceptors improves the charge separation yield, causing significant enhancement of the production of $^\bullet$OH [4–6]. The photocatalytic reactions occurring on semiconductors are characterized by two parallel mechanisms involving reduction and oxidation. The addition of radical precursors (e.g., H_2O_2, IO_4^-, and $S_2O_8^{2-}$) induces the cathodic processes to generate oxidizing species, contributing to the photocatalytic oxidation of aquatic organic contaminants [7,8].

Tungsten oxide (WO₃) with a band gap sufficiently narrow for visible light absorption (i.e., 2.6 eV) has the proper energy level of valence band (i.e., +3.1 V_{NHE}) for oxidation of absorbed water or hydroxide ions into $^\bullet$OH, providing the potential capability for visible-light-induced water treatment and disinfection [9,10]. However, the conduction band (CB) potential (i.e., +0.4 V_{NHE}) of WO₃ is not negative enough to reduce molecular oxygen as an electron acceptor ubiquitously present in aqueous environmental media. As a result, photocatalytic reactions on pure WO₃ are limited due to the rapid recombination of electron–hole pairs. The strategies to enable WO₃ to harness visible light for pollutant oxidation by facilitating charge separation include (1) application of electron acceptors alternative to O_2 (e.g., Cu(II), $S_2O_8^{2-}$) [4,7], (2) loading of co-catalyst (e.g., CuO, Pt) [9,11,12], and (3) coupling of semiconductors with different band-gap structures [13,14]. For example, Cu(II) ions function as electron scavengers to retard the recombination of charge carriers, resulting in a two to three orders of magnitude improvement in the WO₃ photocatalytic

mineralization of methanol [4]. Surface platinization provides a reaction pathway for O_2 reduction via multiple electron transfer, noticeably increasing visible light activity for the oxidation of organic compounds relative to bare WO_3 [9,11].

A combination with the Fenton-like reagent (Fe(III) and H_2O_2) increases the photocatalytic oxidation efficacy of TiO_2 through (1) improved charge separation based on the roles of Fe(III) and H_2O_2 as electron acceptors, (2) reductive conversion of H_2O_2 to •OH via CB electrons, and (3) photo-reduction of Fe(III) for the *in situ* generation of Fe(II) available for Fenton oxidation [5]. The synergistic enhancement is expected for the photocatalytic oxidation by WO_3 in the presence of Fenton-like reagent, because the CB edge potential allows interfacial transfer of CB electrons to Fe(III) and H_2O_2 to enable the catalytic cycle involving Fe(II)/Fe(III) and decomposition of H_2O_2 to yield •OH. In particular, in that visible light irradiation of WO_3 initiates the photo-induced formation of electron–hole pairs, an improvement in photocatalytic degradation through the integration of WO_3 with Fenton-like reagent should be achievable with visible light, offering the potential advanced opportunity for energy-efficient oxidation processes.

This study evaluates the synergistic enhancement of the photocatalytic degradation of diverse organic compounds through the combination of WO_3 photocatalysis with Fenton-like oxidation. The effects of reaction parameters (e.g., Fe(III) and H_2O_2 dosages, and initial pH) on the oxidative degradation kinetics and mechanisms are investigated with both WO_3/H_2O_2 and $WO_3/Fe(III)/H_2O_2$ systems. The photolytic experiments using various probe compounds identify the photo-generated oxidant responsible for accelerated photocatalytic degradation at circumneutral pH. We compare the photocatalytic oxidation efficacy of the ternary combined systems involving pure WO_3 versus surface-modified WO_3, such as platinized WO_3 (Pt-WO_3) and Nafion-coated WO_3 (Nf–WO_3). The visible light activity of the integrated system is accessed based on the potential catalytic performance for degradation of 4-chlorophenol under visible light irradiation, in the presence of a 400-nm UV cut-off filter.

2. Materials and methods

2.1. Reagents

Chemicals that were used as received in this study include: tungsten oxide (WO_3, nanopowder, Aldrich), titanium dioxide (TiO_2, Degussa P25), iron(III) perchlorate hydrate (Aldrich), hydrogen peroxide solution (Sigma–Aldrich), formaldehyde solution (Sigma–Aldrich), p-hydroxybenzoic acid (Aldrich), 4-chlorophenol (Aldrich), phenol (Sigma–Aldrich), bisphenol A (Aldrich), acetaminophen (Aldrich), carbamazepine (Sigma–Aldrich), nitrobenzene (Sigma–Aldrich), benzoic acid (Sigma–Aldrich), 2,4-dinitrophenyl hydrazine (Aldrich), nafion® perfluorinated resin solution (Sigma–Aldrich), methanol (Sigma–Aldrich), 1,10-Penanthroline (Aldrich), phosphoric acid (Aldrich), perchloric acid (Sigma–Aldrich), acetonitrile (J.T. Baker), Ti(IV) sulfate solution (Kanto chemical), and sodium hydroxide solution (Fluka). Deionized water used was ultrapure (18 MΩ cm) and prepared by a Millipore system. All chemicals were of reagent grade and were used without further purification except for 2,4-dinitrophenyl hydrazine (DNPH). DNPH was recrystalized with acetonitrile three times prior to use.

2.2. Photochemical experiments

Photolytic experiments were performed in a magnetically-stirred cylindrical quartz reactor equipped with a 4 W fluorescent lamp (Philips Co.) under air-equilibrated conditions at an ambient temperature ($22 \pm 1\,°C$). The incident light intensity, measured by a pyranometer (Apogee, PYR-P), was determined to be $1.105\,mW/cm^2$. The emission spectrum (350–650 nm) was measured using a spectropro-500 spectrophotometer (Acton Research Co.).

A typical reaction suspension of photocatalyst in combination with Fenton-like reagent was prepared at a concentration of 0.5 g/L photocatalyst, 0.25 mM Fe(III), 5 mM H_2O_2, and 0.1 mM organic compounds. The experimental suspension was un-buffered and air-equilibrated. The initial pH of the suspension was adjusted to a desired value with 1 M $HClO_4$ or NaOH solution. Aliquots of 1 mL were withdrawn at constant time intervals from the photo-irradiated reactor using a 1-mL syringe, were filtered through a 0.45-μm PTFE filter (Millipore), and were injected into a 2-mL amber glass vial containing 20 μL methanol to quench any oxidants that might be generated during the reaction. Experiments were performed at least three times for any given condition. The residual concentrations of target organic substrates were quantitatively analyzed using a HPLC (Shimadzu LC-20AD) equipped with a C-18 column (ZORBAX Eclipse XDB-C18) and a UV/vis detector (SPD-20AV). The HPLC monitoring of 4-chlorophenol was performed using a binary mobile phase of 0.1% (v/v) aqueous phosphoric acid solution and acetonitrile (typically 60: 40 by volume). Fe(II) and H_2O_2 concentrations were measured by the 1,10-phenanthroline method (i.e., $\varepsilon_{510} = 11{,}050\,M^{-1}\,cm^{-1}$) [15] and the titanium sulfate method (i.e., $\varepsilon_{405} = 730\,M^{-1}\,cm^{-1}$) [16], respectively. The concentration of Fe(II) generated by the photocatalytic reduction of Fe(III) was quantified by *in situ* monitoring the evolution of absorbance at 510 nm in a WO_3/Fe(III) suspension containing 1,10-phenanthroline.
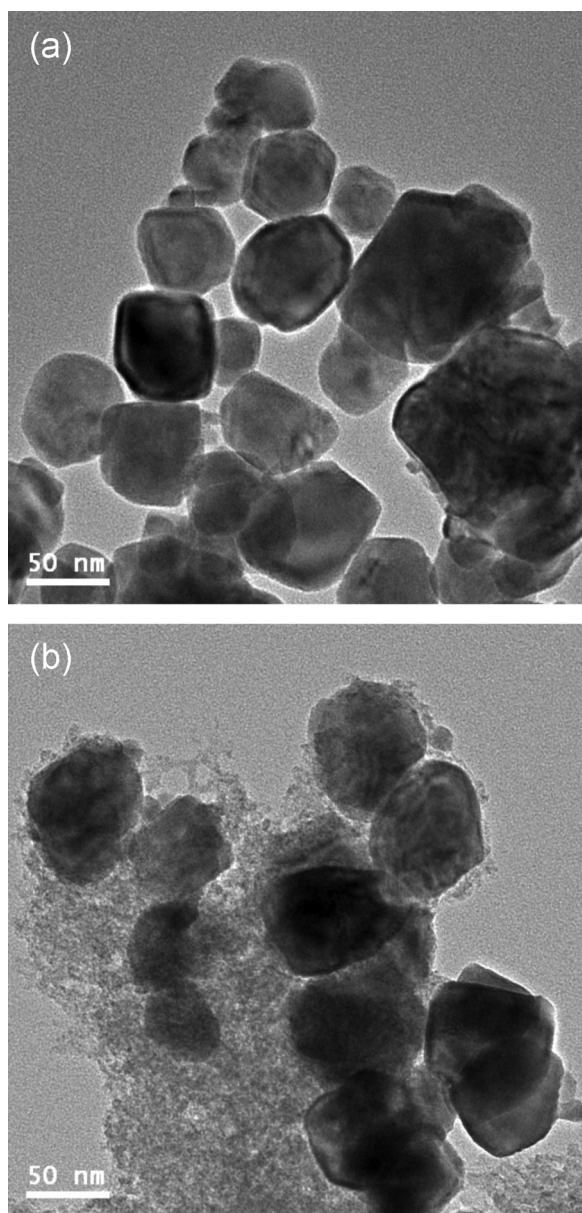
2.3. Characterization of WO_3 nanoparticles

The morphology of bare WO_3 and WO_3 recovered after the photocatalytic reaction in combination with Fenton-like reagent was investigated using a JEOL JEM 2100F high resolution transmission electron microscope (HR-TEM). Fig. 1a shows that pristine WO_3 particulates with the size of 50–100 nm are typically spherical in shape and tend to aggregate in aqueous phase. TEM image of the recovered WO_3 confirms the partial coverage of iron oxyhydroxide precipitates on WO_3 surface (Fig. 1b). Iron content on the recovered WO_3 was determined to be ca. 3 wt% based on the surface chemical composition identified by HR-TEM equipped with an energy dispersive X-ray spectrometer (EDS) (Supplementary Data, Fig. S1). EDS elemental mapping (Supplementary Data, Fig. S2) reveals that the combination with Fenton-like reagent under neutral pH condition causes relatively uniform dispersion of iron oxyhydroxides on WO_3 surface.

2.4. Preparation of platinized and Nafion-coated photocatalysts

Platinization of WO_3 was performed using a photodeposition method [9,17]. An aqueous suspension of WO_3 (0.5 g/L), containing 1 M methanol (electron donor) and 0.1 mM chloroplatinic acid (H_2PtCl_6), was illuminated with a 200-W mercury lamp for 30 min. After photo-irradiation, Pt-WO_3 powder was collected from the resultant suspension of Pt-WO_3 by filtration (0.45 μm membrane filter), washed with Milli-Q water, and dried at 60 °C in a thermostat oven. A typical Pt loading on WO_3 was estimated to be ca. 0.5 wt% through quantification of the concentration of unused chloroplatinic acid remaining in the filtrate solution after photodeposition by atomic absorption spectrometry.

Nafion solution was prepared according to the previously published procedure [18]. 20 mL of 5 wt% Nafion solution (in a mixture of alcohol and water) was added to 300 mL of Milli-Q water. The solution was evaporated at 70–80 °C on a hot-plate until

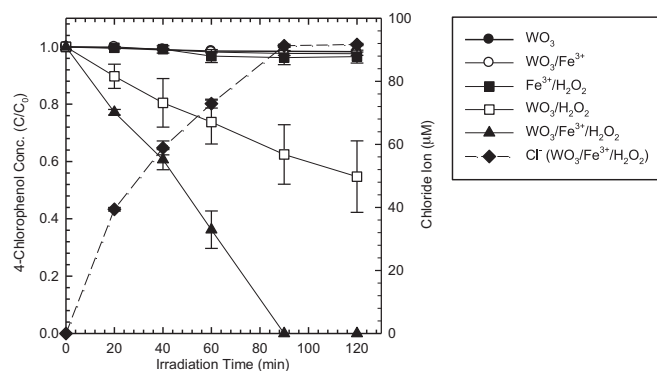**Fig. 1.** TEM images of (a) pristine WO_3 and (b) WO_3 recovered after the use for photocatalytic degradation of 4-CP in conjunction with Fenton-like reagent ($[WO_3]_0 = 0.5$ g/L; $[Fe(III)]_0 = 0.25$ mM; $[H_2O_2]_0 = 5.0$ mM; $[4\text{-}CP]_0 = 0.1$ mM; $pH_i = 7.0$).

the volume was reduced to ca. 50 mL, and then diluted to 300 mL. This procedure was repeated three times to ensure the elimination of residual aliphatic alcohols. WO_3 powder was thoroughly mixed to the appropriate volume of the resultant aqueous Nafion solution (8.3 mg-Nafion/g-WO_3), and was subsequently dried at 80 °C in an oven overnight to obtain Nf-WO_3 powder.

2.5. Identification of reactive oxidants

Methanol, benzoic acid, and coumarin were employed as probe compounds for detecting reactive oxidants. The photolytic experiments were conducted in the presence of excess amounts of probe compounds (200 mM methanol, 10 mM benzoic acid, and 1 mM coumarin) to ensure that all of the reactive oxidants were scavenged by the probe compounds. Formaldehyde (HCHO) and p-hydroxybenzoic acid (pHBA) as the predominant products generated during the photocatalytic oxidation of methanol and benzoic

Fig. 2. Photocatalytic degradation of 4-CP and production of chloride ions in systems of WO_3, $WO_3/Fe(III)$, $Fe(III)/H_2O_2$, WO_3/H_2O_2, and $WO_3/Fe(III)/H_2O_2$ under fluorescent light irradiation ($[WO_3]_0 = 0.5$ g/L; $[Fe(III)]_0 = 0.25$ mM; $[H_2O_2]_0 = 5.0$ mM; $[4\text{-}CP]_0 = 0.1$ mM; $pH_i = 7.0$).

acid were quantified using the HPLC. 7-hydroxycoumarin, a product of photocatalytic coumarin oxidation, was determined by monitoring the fluorescence emission at 460 nm under excitation at 332 nm using a spectrofluorometer (Shimadzu RF-5301).
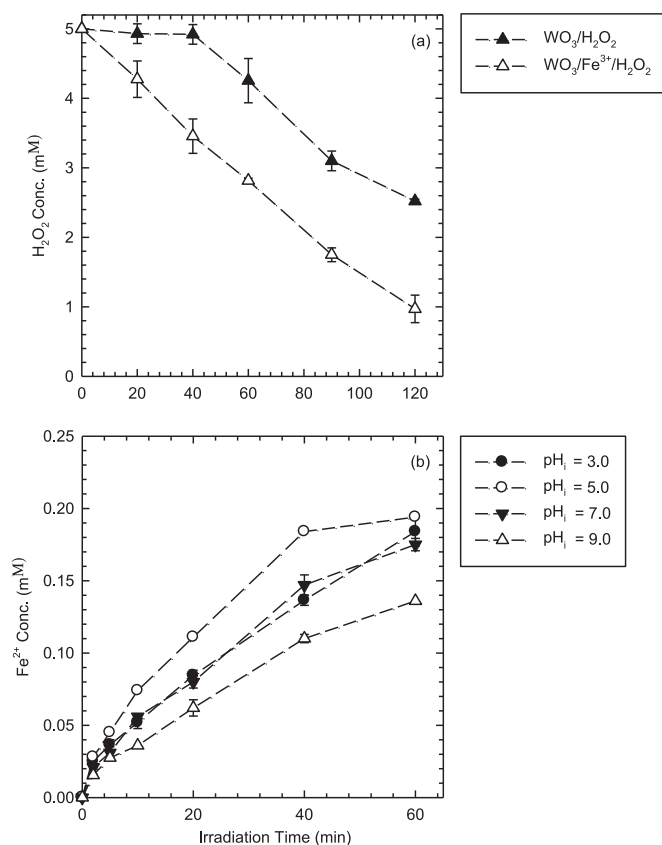
3. Results and discussion

3.1. Enhanced photocatalytic degradation of 4-chlorophenol in the $WO_3/Fe(III)/H_2O_2$ system

In order to explore the potential synergistic combination, the kinetics for the photocatalytic degradation of 4-chlorophenol (4-CP) was monitored in the systems of $Fe(III)/H_2O_2$, WO_3, $WO_3/Fe(III)$, WO_3/H_2O_2, and $WO_3/Fe(III)/H_2O_2$ under fluorescent light irradiation (Fig. 2). The solution was initially adjusted to pH 7.0, which was gradually decreased to approximately 4.3 during the course of photocatalytic degradation (Supplementary Data, Fig. S3). Sorption in the dark condition and direct photolysis with fluorescent light did not cause any detectable loss of 4-CP (data not shown). Degradation of 4-CP by WO_3 alone under fluorescent light irradiation was completely absent (Fig. 2), which assures that WO_3 is not capable of photocatalytic oxidation due to the non-utilization of O_2 as an electron acceptor. While the presence of Fe(III) enhanced the photocatalytic degradation of 4-CP at acidic pH (Supplementary Data, Fig. S4), low aqueous solubility of Fe(III) under weakly acidic and neutral pH conditions appeared to inhibit the role of Fe(III) as an electron scavenger, resulting in negligible 4-CP oxidation in the $WO_3/Fe(III)$ system (Fig. 2). Unlike the very rapid Fenton-like reaction which took place at an initial pH of 3 (Supplementary Data, Fig. S4), the $Fe(III)/H_2O_2$ suspension which was initially adjusted to pH 7 did not degrade any detectable amount of 4-CP (Fig. 2).

The addition of H_2O_2 to the aqueous WO_3 suspension (i.e., the WO_3/H_2O_2 system) led to the increased photocatalytic oxidation of 4-CP relative to pure WO_3 (Fig. 2). In particular, despite the negligible activity of Fe(III) as an electron acceptor under neutral pH condition, the kinetic enhancement of the photocatalyzed degradation of 4-CP was more significant in the presence of both Fe(III) and H_2O_2 (i.e., the $WO_3/Fe(III)/H_2O_2$ system), based on the pseudo first-order rate constants (0.0052 min^{-1} for WO_3/H_2O_2; 0.0155 min^{-1} for $WO_3/Fe(III)/H_2O_2$). Stoichiometric chloride production, as a direct indication of dechlorination, confirms that the rapid 4-CP disappearance should be ascribed to the increased oxidizing capacity of the $WO_3/Fe(III)/H_2O_2$ combined system. On the other hand, the notable synergistic enhancement in photocatalytic efficacy did not occur in integrated ternary systems involving TiO_2 under neutral pH conditions (Supplementary Data, Fig. S5). The kinetic comparison of the combined systems using WO_3 and TiO_2 demonstrates
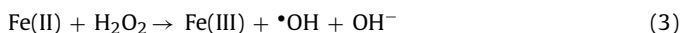
Fig. 3. (a) H_2O_2 decomposition in the WO_3/H_2O_2 and $WO_3/Fe(III)/H_2O_2$ systems ($[WO_3]_0 = 0.5$ g/L; $[Fe(III)]_0 = 0.25$ mM; $[H_2O_2]_0 = 5.0$ mM; $[4\text{-}CP]_0 = 0.1$ mM; $pH_i = 7.0$) and (b) production of Fe(II) in the $WO_3/Fe(III)$ system at various pH values under fluorescent light irradiation ($[WO_3]_0 = 0.5$ g/L; $[Fe(III)]_0 = 0.25$ mM; $[1.10\text{-phenantrolin}]_0 = 10$ mM; $pH_i = 3.0, 5.0, 7.0, 9.0$).

that improvement in photocatalytic performance through the combination with Fenton-like reagent is more pronounced in aqueous WO_3 suspensions (Fig. 2 and Supplementary Data, Fig. S5).
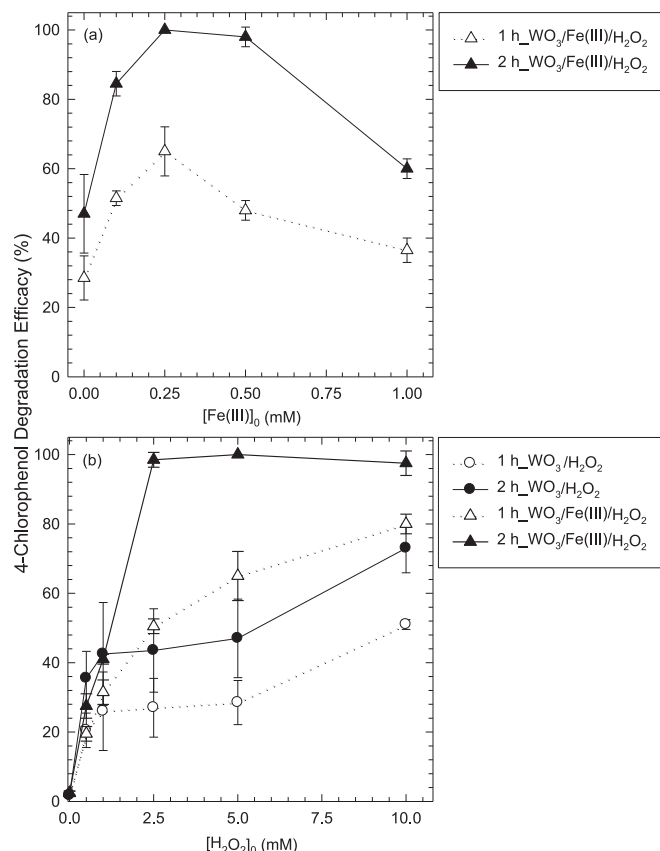
The production of $^{\bullet}OH$ as a result of H_2O_2 reduction by photo-generated CB electron (reaction (1)) leads to significant 4-CP degradation in the WO_3/H_2O_2 system.

$$e_{cb}^- + H_2O_2 \rightarrow {}^{\bullet}OH + OH^- \tag{1}$$

Faster H_2O_2 decomposition in the $WO_3/Fe(III)/H_2O_2$ system relative to the WO_3/H_2O_2 system (Fig. 3a) indicates the possible conversion of H_2O_2 into reactive oxidants in the presence of iron oxyhydroxide precipitates on the WO_3 surface. Fe(II) measurement in the $WO_3/Fe(III)$ system (conducted in order to detect *in situ* generated Fe(II) prior to its oxidation by H_2O_2) showed that the reduction of Fe(III) into Fe(II) on the photo-irradiated WO_3 (reaction (2)) was not retarded at higher initial pH values (Fig. 3b). The significant Fe(II) production from the insoluble Fe(III) precipitate predominantly occurs at initial pH 7 (not filterable with a 0.45 μm syringe filter), as well as a more favorable reduction of H_2O_2 in the ternary combined system, imply that the kinetic enhancement in the $WO_3/Fe(III)/H_2O_2$ system may be attributed to the production of $^{\bullet}OH$ via the Fenton reaction (reaction (3)).

$$e_{cb}^- + Fe(III) \rightarrow Fe(II) \tag{2}$$

$$Fe(II) + H_2O_2 \rightarrow Fe(III) + {}^{\bullet}OH + OH^- \tag{3}$$

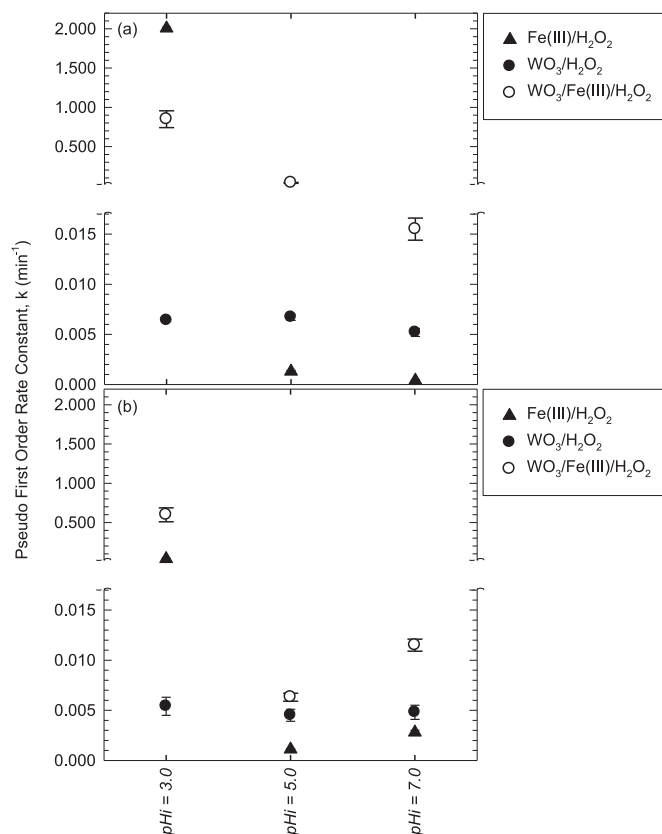The capture of CB electrons by Fe(III) (evidenced by the photoreduction of Fe(III) into Fe(II) in Fig. 3b) can facilitate a

charge separation and subsequently improve the conversion of adsorbed water or hydroxide ions to $^{\bullet}OH$ via VB hole (reaction (4)).

$$h_{vb}^+ + H_2O \rightarrow {}^{\bullet}OH + H^+ \tag{4}$$

However, 4-CP degradation in the $WO_3/Fe(III)$ system was absent (Fig. 2), which indicates that the electron scavenging action of iron oxide precipitates does not significantly enhance $^{\bullet}OH$ production through the oxidation of water/hydroxide molecules by VB hole. The negligible acceleration in photocatalytic oxidative degradation in the presence of efficient interfacial CB electron transfer has also been observed in platinized WO_3 photocatalysis, in which a platinum deposit, as a co-catalyst, promotes the multiple CB electron transfer to reductively convert O_2 to H_2O_2 [9]. As an alternative hypothesis, the redox cycling of iron could mediate a recombination path in which adsorbed iron species react sequentially with trapped electrons and holes.

3.2. Effects of Fe(III) and H_2O_2 concentration and initial pH

The photocatalytic degradation of 4-CP in both WO_3/H_2O_2 and $WO_3/Fe(III)/H_2O_2$ systems was performed with varying initial concentrations of Fe(III) and H_2O_2 (Fig. 4a and b). The 4-CP degradation efficacy was enhanced with increasing the initial Fe(III) concentration up to 0.25 mM (Fig. 4a) because Fenton reaction involving Fe(II) (*in situ* generated through CB electron transfer to Fe(III)) is kinetically favored at high Fe(III) concentrations. However, iron loading higher than 0.25 mM caused a gradual drop in the degradation efficacy (Fig. 4a), which is probably attributed to the further
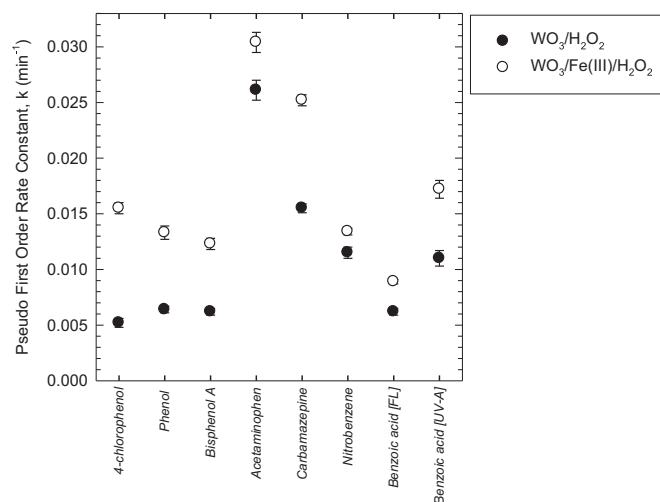

Fig. 4. Photocatalytic degradation of 4-CP by (a) the $WO_3/Fe(III)/H_2O_2$ system as a function of initial Fe(III) concentration ($[WO_3]_0 = 0.5$ g/L; $[Fe(III)]_0 = 0.1, 0.25, 0.5,$ and 1.0 mM; $[H_2O_2]_0 = 5.0$ mM; $[4\text{-}CP]_0 = 0.1$ mM; $pH_i = 7.0$) and (b) the WO_3/H_2O_2 and the $WO_3/Fe(III)/H_2O_2$ systems as a function of initial H_2O_2 concentration ($[WO_3]_0 = 0.5$ g/L; $[Fe(III)]_0 = 0.25$ mM; $[H_2O_2]_0 = 0.5, 1.0, 2.5, 5.0,$ and 10 mM; $[4\text{-}CP]_0 = 0.1$ mM; $pH_i = 7.0$).

Fig. 5. Pseudo first-order rate constants for (a) photocatalytic degradation of 4-CP and (b) H_2O_2 decomposition in the Fe(III)/H_2O_2, the WO$_3$/H_2O_2 and the WO$_3$/Fe(III)/H_2O_2 systems, as a function of pH ([WO$_3$]$_0$ = 0.5 g/L; [Fe(III)]$_0$ = 0.25 mM; [H_2O_2]$_0$ = 5.0 mM; [4-CP]$_0$ = 0.1 mM; pH$_i$ = 3.0, 5.0, and 7.0).

Fig. 6. Pseudo first-order rate constants for photocatalytic degradation of various organic contaminants in the WO$_3$/H_2O_2 and the WO$_3$/Fe(III)/H_2O_2 systems ([WO$_3$]$_0$ = 0.5 g/L; [Fe(III)]$_0$ = 0.25 mM; [H_2O_2]$_0$ = 5.0 mM; [organic contaminants]$_0$ = 0.1 mM; pH$_i$ = 7.0).

precipitation of iron oxyhydroxides on the catalyst surface and the relevant decrease in photon absorption by WO$_3$. The effect of initial Fe(III) concentration on photocatalytic activity was similarly observed in the combined system using TiO$_2$ [5]. Fig. 4b shows that the presence of H_2O_2 at higher concentrations caused a more effective photocatalytic degradation in the WO$_3$/H_2O_2 and WO$_3$/Fe(III)/H_2O_2 systems. The photocatalytic performance difference between the binary and ternary systems was negligible at low initial H_2O_2 concentrations. On the other hand, when the applied H_2O_2 concentration reached 2.5 to 10 mM, the efficacy of 4-CP degradation by the WO$_3$/Fe(III)/H_2O_2 system approached a maximum, which was significantly higher compared to that of the WO$_3$/H_2O_2 system.

Fig. 5a and b shows the rates of 4-CP degradation and H_2O_2 decomposition in the systems of Fe(III)/H_2O_2, WO$_3$/H_2O_2 and WO$_3$/Fe(III)/H_2O_2, as a function of initial pH. Acidic conditions favored both 4-CP degradation and H_2O_2 decomposition in the Fe(III)/H_2O_2 and the WO$_3$/Fe(III)/H_2O_2 systems, while the kinetics for 4-CP degradation and H_2O_2 decay in the WO$_3$/H_2O_2 system did not change depending on initial pH. The drastic reduction in photocatalytic activity of the Fe(III)/H_2O_2 and the WO$_3$/Fe(III)/H_2O_2 systems with increasing pH may be due to the low yield of •OH via the Fenton reaction under neutral pH conditions (as discussed in Section 3.4 in more detail).

3.3. Oxidative degradation of various organic contaminants

Fig. 6 compares the pseudo first order rate constants for photocatalytic degradation of diverse organic compounds in the WO$_3$/H_2O_2 and WO$_3$/Fe(III)/H_2O_2 systems. Overall, the presence of Fe(III) caused the more rapid photocatalytic oxidation of all

tested organic compounds. The kinetic enhancement was more pronounced with selected target compounds, including phenol, 4-chlorophenol, bisphenol A, and carbamazepine, while the photocatalytic degradation efficiency was not significantly improved with acetaminophen, benzoic acid and nitrobenzene. The observation that synergistic enhancement varies sensitively depending on target compound could be ascribed to (1) surface affinity of WO$_3$ (or iron-loaded WO$_3$) with substrate specificity and (2) degradation mechanism involving selective oxidants (e.g., ferrly ion (Fe(IV)) formed via the Fenton reaction at circumneutral pH.

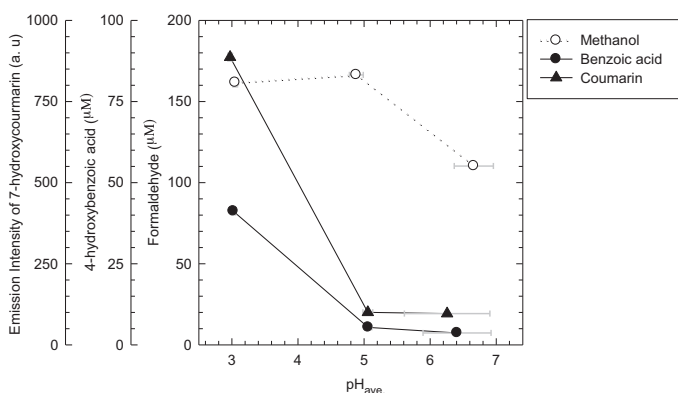### 3.4. Nature of reactive oxidants produced by the WO$_3$/Fe(III)/H_2O_2 system

It is well recognized that one electron reduction of H_2O_2 by Fe(II) initiates •OH generation in the Fenton reaction (reaction (3)). However, two-electron transfer from Fe(II) to H_2O_2 produces the ferryl ion as a non-radical transient intermediate (reaction (5)), mediating the alternative pathway for oxidation of organic compounds.

$$Fe(II) + H_2O_2 \rightarrow Fe(IV) + 2OH^- \tag{5}$$

Whereas •OH functions as the primary oxidant in the Fenton reagent-induced organic oxidation performed under acidic pH condition, a role of Fe(IV) becomes more significant with increasing pH [19–21]. The presence of ligands (e.g., oxalate, nitrilotriacetate and polyoxometalates) or metal oxide matrices (e.g., silica–alumina composite, TiO$_2$) modifies the electron transfer mechanism of the Fenton reaction, enhancing Fe(II)-catalyzed conversion of H_2O_2 to •OH under neutral pH conditions [5,22,23].

In order to identify the reactive oxidants generated by the WO$_3$/Fe(III)/H_2O_2 system, the photocatalytic oxidation of three probe compounds (i.e., methanol, benzoic acid, and coumarin) was examined as a function of initial pH (Fig. 7). The oxidative conversion of methanol (susceptible to oxidation by Fe(IV) as well as •OH) to formaldehyde [21,24] in the WO$_3$/Fe(III)/H_2O_2 system was not notably inhibited as the initial pH increased. On the other hand, the efficacy for production of 4-hydroxybenzoic acid (or 7-hydroxylcoumarin) (i.e., hydroxylation of benzoic acid (or coumarin) as an indirect probe for •OH production [25,26]) was drastically retarded with increasing pH. The results indicate that acidic pH conditions favor the generation of •OH in the ternary system, while a significant oxidation pathway involving Fe(IV)
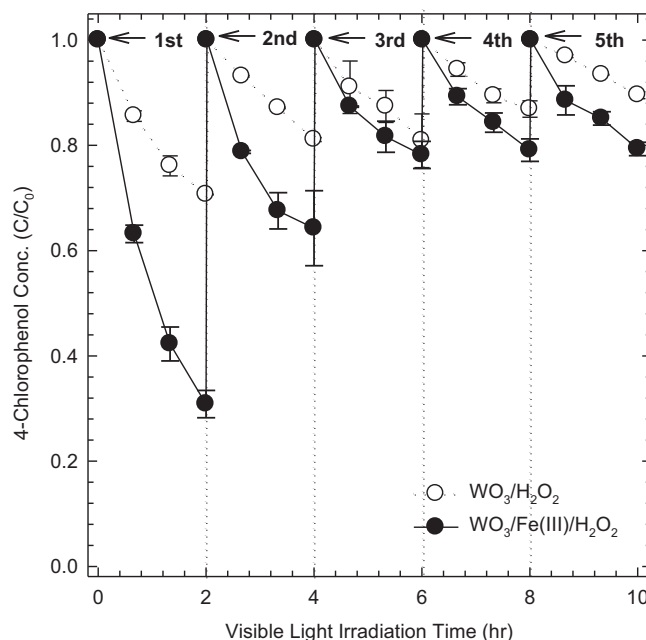
Fig. 7. Production of formaldehyde, 4-hydroxybenzoic acid (4-HBA), and 7-hydroxycoumarin in the presence of methanol, benzoic acid, and coumarin in the $WO_3/Fe(III)/H_2O_2$ system ($[WO_3]_0 = 0.5$ g/L; $[Fe(III)]_0 = 0.25$ mM; $[H_2O_2]_0 = 5.0$ mM; $[methanol]_0 = 200$ mM; $[benzoic\ acid]_0 = 10$ mM; $[coumarin]_0 = 1$ mM; $pH_i = 3.0, 5.0,$ and 7.0).

is present under neutral pH conditions. Contrary to a significant loss of photocatalytic activity of the $WO_3/Fe(III)/H_2O_2$ system for production of OH radical under neutral pH conditions, reductive conversion of Fe(III) to Fe(II) and subsequent electron transfer reaction of Fe(II) with H_2O_2 on the photoexcited TiO_2 surface lead to generation of OH radical as the dominant reactive intermediate at circumneutral pH [5]. Benzoic acid (or coumarin) hydroxylation efficacy and photocatalytic 4-CP degradation rate show a similar pH dependency, which implies a role of $^{\bullet}OH$ as the main oxidant in the photocatalytic oxidation of 4-CP in the $WO_3/Fe(III)/H_2O_2$ system.

3.5. Effect of surface modification

The photocatalytic oxidation of 4-CP was carried out in ternary combined systems involving surface-modified WO_3 including $Pt–WO_3$ ($Pt–WO_3/Fe(III)/H_2O_2$) and $Nf–WO_3$ ($Nf–WO_3/Fe(III)/H_2O_2$) (Fig. 8). Surface platinization enables H_2O_2 formation and its subsequent reduction to $^{\bullet}OH$ on the WO_3 surface, through multiple electron transfer to O_2 [9,11]. As WO_3 coated with negatively-charged Nafion polymer exhibits an improved surface affinity toward cationic organics, the photocatalytic oxidative degradation via free $^{\bullet}OH$ can be facilitated in the presence of hydrophobic Nafion layers that exclude water molecules from the proximity of the WO_3 surface [27,28]. Despite the possible scenarios for kinetic enhancement in photocatalytic
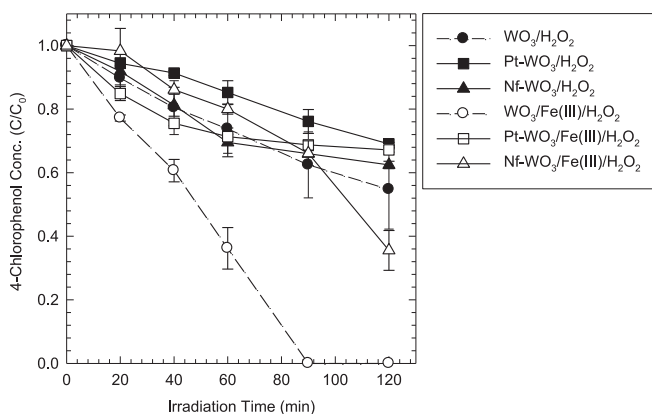

Fig. 8. Effects of surface modification on photocatalytic degradation of 4-CP by the WO_3/H_2O_2 and the $WO_3/Fe(III)/H_2O_2$ systems ($[WO_3]_0 = [Pt–WO_3]_0 = [Nf–WO_3]_0 = 0.5$ g/L; $[Fe(III)]_0 = 0.25$ mM; $[H_2O_2]_0 = 5.0$ mM; $[4-CP]_0 = 0.1$ mM; $pH_i = 7.0$).

Fig. 9. Repeated degradation of 4-CP by the WO_3/H_2O_2 and the $WO_3/Fe(III)/H_2O_2$ systems under visible light irradiation (>400 nm) ($[WO_3]_0 = 0.5$ g/L; $[Fe(III)]_0 = 0.25$ mM; $[H_2O_2]_0 = 5.0$ mM; $[4-CP]_0 = 0.1$ mM; $pH_i = 7.0$).

oxidation on surface-modified WO_3, the combination with Fenton-like reagent did not accelerate photocatalytic 4-CP degradation by $Pt–WO_3$ and $Nf–WO_3$ (compared to the systems of $Pt–WO_3/H_2O_2$ and $Nf–WO_3/H_2O_2$), which was in marked contrast to the combined system using bare WO_3 (Fig. 8). The negligible performance improvement of the $Pt–WO_3/Fe(III)/H_2O_2$ and $Nf–WO_3/Fe(III)/H_2O_2$ systems indicates that the presence of platinum deposits or Nafion coatings as physical barriers hinders the precipitation of Fe(III) as iron oxide form on the WO_3 surface, preventing the significant photo-reduction of Fe(III) to Fe(II) and the associated production of $^{\bullet}OH$ via the Fenton reaction.

3.6. Repetition test under visible light irradiation

Photocatalytic 4-CP degradation by the WO_3 (or TiO_2)/H_2O_2 and the WO_3 (or TiO_2)/$Fe(III)/H_2O_2$ systems was repeated over five cycles (performed in the same batch with injecting 100 μM 4-CP and 5 mM H_2O_2 every 2 h) under visible light irradiation (Fig. 9 and Supplementary Data, Fig. S6). The WO_3/H_2O_2 and $WO_3/Fe(III)/H_2O_2$ systems caused significant 4-CP degradation (see the first cycle in the repetition test) (Fig. 9), while TiO_2 (known to exhibit no visible light activity) negligibly degraded 4-CP either in the presence of H_2O_2 or in combination with Fenton-like reagent (Supplementary Data, Fig. S6). The slight 4-CP degradation (less than 10%) by the TiO_2/H_2O_2 and $TiO_2/Fe(III)/H_2O_2$ systems in the first cycle is likely ascribed to the formation of a visible-light-absorbing $TiO_2–H_2O_2$ surface complex [29]. The kinetically enhanced oxidation in the $WO_3/Fe(III)/H_2O_2$ system (relative to the WO_3/H_2O_2 system) was observed under visible light irradiation (Fig. 9). The photocatalytic activity of the $WO_3/Fe(III)/H_2O_2$ system for 4-CP degradation, though considerably decreased over two initial cycles, was maintained to a certain degree after the third cycle batch run. The possible loss of WO_3 from periodic sampling, and undesirable consumption of $^{\bullet}OH$ by accumulated oxidation products, may be responsible for the gradual reduction in the photocatalytic degradation efficacy.

4. Conclusions

This study demonstrated that the combination with Fenton-like reagent drastically accelerated WO_3-mediated photocatalytic oxidation under initially neutral pH conditions that favor the precipitation of Fe(III)-oxyhydroxides. Although significant photo-reduction of Fe(III) to Fe(II) took place on WO_3 irrespective of pH conditions, the inability of Fe(III) as an electron scavenger to facilitate charge separation at neutral pH was confirmed based on the negligible oxidative degradation in the WO_3/Fe(III) system. On the other hand, the photo-generation of Fe(II) led to more rapid H_2O_2 decomposition in the WO_3/Fe(III)/H_2O_2 system (relative to the WO_3/H_2O_2 system), implying the possible involvement of the Fenton reaction in the enhanced photocatalytic degradation. The photolytic experiments with various probe compounds (benzoic acid, coumarin, and methanol) showed that the WO_3/Fe(III)/H_2O_2 system was more photoactive for the production of both $^\bullet OH$ and Fe(IV) than the WO_3/H_2O_2 system. The efficacy for hydroxylation of benzoic acid and coumarin (as $^\bullet OH$ probe) correlated well to the rate of photocatalytic 4-CP oxidation, as initial pH of the aqueous suspensions of WO_3/Fe(III)/H_2O_2 increased, indicating that Fe(II)-mediated conversion of H_2O_2 to $^\bullet OH$ is responsible for the improved photocatalytic activity of the ternary system for organic oxidation. In addition to the iron-catalyzed decomposition of H_2O_2 to produce $^\bullet OH$ at circum-neutral pH, significant oxidative degradation under visible light irradiation was achieved in the WO_3/Fe(III)/H_2O_2 system, suggesting the potential application as a viable strategy to enable visible-light-driven water treatment operational at a broad range of pH.

Acknowledgements

Appendix A. Supplementary data

Supplementary data associated with this article can be found, in the online version, at http://dx.doi.org/10.1016/j.apcatb.2013.03.006.

References

[1] M.R. Hoffmann, S.T. Martin, W.Y. Choi, D.W. Bahnemann, Chemical Reviews 95 (1995) 69–96.
[2] D.F. Ollis, E. Pelizzetti, N. Serpone, Environmental Science and Technology 25 (1991) 1522–1529.
[3] A. Mills, S. LeHunte, Journal of Photochemistry and Photobiology A: Chemistry 108 (1997) 1–35.
[4] T. Arai, M. Yanagida, Y. Konishi, A. Ikura, Y. Iwasaki, H. Sugihara, K. Sayama, Applied Catalysis B: Environmental 84 (2008) 42–47.
[5] H.E. Kim, J. Lee, H. Lee, C. Lee, Applied Catalysis B: Environmental 115 (2012) 219–224.
[6] R.R. Ozer, J.L. Ferry, Environmental Science and Technology 35 (2001) 3242–3246.
[7] W. Chu, Y.F. Rao, Chemosphere 86 (2012) 1079–1086.
[8] A. Muneer, J. Theurich, D. Bahnemann, Journal of Photochemistry and Photobiology A: Chemistry 143 (2001) 213–219.
[9] J. Kim, C.W. Lee, W. Choi, Environmental Science and Technology 44 (2010) 6849–6854.
[10] K. Sayama, H. Hayashi, T. Arai, M. Yanagida, T. Gunji, H. Sugihara, Applied Catalysis B: Environmental 94 (2010) 150–157.
[11] R. Abe, H. Takami, N. Murakami, B. Ohtani, Journal of the American Chemical Society 130 (2008) 7780–7781.
[12] T. Arai, M. Horiguchi, M. Yanagida, T. Gunji, H. Sugihara, K. Sayama, Journal of Physical Chemistry C 113 (2009) 6602–6609.
[13] X.Z. Li, F.B. Li, C.L. Yang, W.K. Ge, Journal of Photochemistry and Photobiology A: Chemistry 141 (2001) 209–217.
[14] C.F. Lin, C.H. Wu, Z.N. Onn, Journal of Hazardous Materials 154 (2008) 1033–1039.
[15] H. Tamura, K. Goto, YotsuyanT., M. Nagayama, Talanta 21 (1974) 314–318.
[16] G.M. Eisenberg, Industrial and Engineering Chemistry 15 (1943) 327–328.
[17] J. Lee, H. Park, W. Choi, Environmental Science and Technology 36 (2002) 5462–5468.
[18] W. Kim, T. Seok, W. Choi, Energy and Environmental Science 5 (2012) 6066–6070.
[19] S.J. Hug, L. Canonica, M. Wegelin, D. Gechter, U. Von Gunten, Environmental Science and Technology 35 (2001) 2114–2121.
[20] S.J. Hug, O. Leupin, Environmental Science and Technology 37 (2003) 2734–2742.
[21] C.R. Keenan, D.L. Sedlak, Environmental Science and Technology 42 (2008) 1262–1267.
[22] C.R. Keenan, D.L. Sedlak, Environmental Science and Technology 42 (2008) 6936–6941.
[23] C. Lee, C.R. Keenan, D.L. Sedlak, Environmental Science and Technology 42 (2008) 4921–4926.
[24] L.Z. Sun, J.R. Bolton, Journal of Physical Chemistry 100 (1996) 4127–4134.
[25] K. Ishibashi, A. Fujishima, T. Watanabe, K. Hashimoto, Electrochemistry Communications 2 (2000) 207–210.
[26] X.L. Zhou, K. Mopper, Marine Chemistry 30 (1990) 71–88.
[27] J. Lee, W.Y. Choi, J. Yoon, Environmental Science and Technology 39 (2005) 6800–6807.
[28] H. Park, W. Choi, Journal of Physical Chemistry B 109 (2005) 11667–11674.
[29] X.Z. Li, C.C. Chen, J.C. Zhao, Langmuir 17 (2001) 4118–4122.